Title

Sulfotransferase 1C2 Increases Mitochondrial Respiration by Converting Mitochondrial Membrane Cholesterol to Cholesterol Sulfate.

Journal

Biochemistry, 63(18)

Authors

Kolb, Alexander

Corridon, Peter

Ullah, Mahbub

et al.

Publication Date

2024-09-17

DOI

10.1021/acs.biochem.3c00344

Peer reviewed

Biochemistry

pubs.acs.org/biochemistry
Article

Sulfotransferase 1C2 Increases Mitochondrial Respiration by Converting Mitochondrial Membrane Cholesterol to Cholesterol Sulfate

Alexander J. Kolb, Peter Corridon, Mahbub Ullah, Zechariah J. Pfaffenberger, Wei Min Xu, Seth Winfree, Ruben H. Sandoval, Takeshi Hato, Frank A. Witzmann, Rodrigo Mohallem, Jackeline Franco, Uma K. Aryal, Simon J. Atkinson, David P. Basile,[‡‡] and Robert L. Bacallao*[,‡‡]

Cite This: *Biochemistry* 2024, 63, 2310−2322

ABSTRACT: Hypothesis: In this communication, we test the hypothesis that sulfotransferase 1C2 (SULT1C2, UniProt accession no. Q9WUW8) can modulate mitochondrial respiration by increasing state-III respiration. Methods and results: Using freshly isolated mitochondria, the addition of SULT1C2 and 3-phosphoadenosine 5 phosphosulfate (PAPS) results in an increased maximal respiratory capacity in response to the addition of succinate, ADP, and rotenone. Lipidomics and thin-layer chromatography of mitochondria treated with SULT1C2 and PAPS showed an increase in the level of cholesterol sulfate. Notably, adding cholesterol sulfate at nanomolar concentration to freshly isolated mitochondria also increases maximal respiratory capacity. In vivo studies utilizing gene delivery of SULT1C2 expression plasmids to kidneys result in increased mitochondrial membrane potential and confer resistance to ischemia/reperfusion injury. Mitochondria isolated from gene-transduced kidneys have elevated state-III respiration as compared with controls, thereby recapitulating results obtained with mitochondrial fractions treated with SULT1C2 and PAPS. Conclusion: SULT1C2 increases mitochondrial respiratory capacity by modifying cholesterol, resulting in increased membrane potential and maximal respiratory capacity. This finding uncovers a unique role of SULT1C2 in cellular physiology and extends the role of sulfotransferases in modulating cellular metabolism.

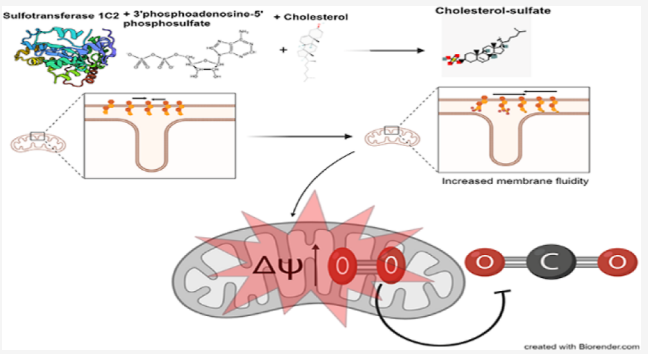

INTRODUCTION

Ischemic preconditioning (IPC) confers organ-level protection against subsequent ischemic episodes. The phenomenon was first described by Murry who showed that a series of brief bouts of ischemia brought about by coronary artery occlusion conferred protection against a subsequent bout of prolonged coronary artery occlusion.[1] Since that ground breaking study, the observation was extended to other organs and methods of inducing preconditioning.[2] Most notably, subjecting a limb to ischemia has been demonstrated to convey distal target organ resistance to injury.[3−5] Despite these promising laboratory observations, it has been difficult to demonstrate a clinical effect with IPC as reports from many studies using multiple different approaches have had widely varying outcomes.[6,7]

There are two signaling pathways mediating IPC: the RISK and SAFE pathways.[6] The survival activating factor enhancement (SAFE) pathway is associated with remote ischemia preconditioning, while the reperfusion injury salvage kinase (RISK) pathway directs the tissue responses to local ischemia.[8] Both pathways alter mitochondrial physiology, which, among other cellular adaptations, results in cellular resistance to ischemia.[9] While both pathways appear to confer short-term resistance to subsequent ischemia, long-term cellular adaptations are poorly understood.

To garner insights into changes in mitochondrial composition that are related to the long-term IPC response, we performed proteomic surveys on mitochondria isolated 14 days after kidney IPC.[10] We found 12 mitochondrial proteins that were significantly increased in the ischemic preconditioned state. Some proteins identified in the proteomics screen appeared to have seemingly irrelevant roles in modifying mitochondria. One such protein is sulfotransferase 1C2 (SULT1C2), a cytosolic enzyme that covalently attaches

Received: July 1, 2023
Revised: August 16, 2024
Accepted: August 21, 2024
Published: August 28, 2024

https://doi.org/10.1021/acs.biochem.3c00344
Biochemistry 2024, 63, 2310−2322

sulfate moieties to target molecules such as androgens, thyroid hormone, xenobiotics, and lipids.[11,12] However, due to the sharp increase in mitochondrial expression of SULT1C2, we hypothesized that this enzyme may play a previously unappreciated role in mitochondrial physiology and could play an important role in the preconditioned state. In this letter, we show that SULT1C2 directly modifies mitochondrial physiology and contributes to a renal protective effect against ischemic injury in the absence of prior preconditioning.

MATERIALS AND METHODS

Materials. All fluorescent probes were purchased from Thermo Fisher Scientific (Waltham, MA). Recombinant SULT1C2 (specific activity >45 pmol/min-ug) was purchased from Novus Biologics (R&D Systems, Minneapolis, MN), 3′-phosphoadenosine 5′-phosphosulfate lithium salt (PAPS) was purchased from Millipore-Sigma (St. Louis, MO), and cholesterol sulfate was purchased from Avanti Polar Lipids, Inc. (Alabaster, AL). SULT1C2 antibody was purchased from Protein Tech (Chicago, IL). Beta actin was purchased from Millipore (Billerica, MA). All secondary antibodies were purchased from Jackson Laboratories (West Grove, PA). Lipofectamine 3000 was purchased from Thermo Fisher Scientific (Waltham, MA). All plasmid DNA was purchased from OriGene (Rockville, MD). Specifically, rat SULT1C2 (NM_133547) tagged with Myc and DKK (clone RR202511) was purchased from OriGene (Rockville, MD). FIJI was downloaded from the NIH Web site (National Institutes of Health, Bethesda, MD).[13]

Animal Care and Use. Male Sprague−Dawley rats (Envigo, Indianapolis, IN) (250−350 g) were used for our in vivo studies. Rats had access to food and water, and all experiments conducted followed NIH guidelines. Rats were randomly assigned to the control or experimental groups. Approval from the Indiana University School of Medicine Institutional Animal Care and Use Committee (IACUC) and Richard L. Roudebush VAMC animal care and use committee was gained prior to all in vivo studies.

IPC, Hydrodynamic Gene Delivery, and Acute Kidney Injury Methods. To induce acute kidney injury, bilateral renal ischemia reperfusion (I/R) was induced by 40 min renal pedicle clamping in rats anesthetized with ketamine (100 mg/kg), xylazine (10 mg/kg), and acepromazine (2.5 mg/kg) cocktail as described previously. Serum creatinine levels were determined from animals with a 24 h postischemia time point used to evaluate the degree of renal dysfunction. IPC was performed by allowing rats to recover from renal I/R for 14 days after serum creatinine levels returned to level observed in sham control animals; and the efficacy of IPC was verified by a second bout of IRI that has been described previously.[14]

To determine the effect of exogenous SULT1C2 in kidney mitochondrial function and response to ischemic injury, plasmid DNA carrying full-length *sult1C2* was delivered into the left kidney by hydrodynamic delivery (300 μg plasmid DNA in 0.5 mL saline), similar to approaches we have described previously.[15] Since the right kidney is more difficult to access, unilateral nephrectomy of the right kidney was conducted such that the only remaining kidney had been subjected to gene delivery. Additional studies using a *LacZ* expressing plasmid (300 μg plasmid DNA in 0.5 mL saline) were used to help identify and confirm the renal tubular segment expression plasmid DNA.[16]

After 1 week of recovery, the effect of exogenous gene delivery to the remaining kidney was evaluated by subjecting rats to ischemia/reperfusion, as outlined above. Assessment of renal damage was evaluated by measuring serum creatinine values at 24 h post ischemia/reperfusion or by histological assessment.

Isolation and Analysis of Mitochondria. Kidney mitochondria were isolated from rats and used for respiration assays or for biochemical and lipidomic studies, as described later. Kidney cortex was homogenized in mitochondrial isolation buffer (250 mM sucrose, 20 mM HEPES, 10 mM KCl, 1.5 mM $MgCl_2$, 1.0 mM EDTA pH 7.9) using a PBI S3 shredder (Pressure Biosciences, Easton, MA). The homogenate was centrifuged at 800*g* for 10 min at 4 °C. The supernatant was collected and centrifuged at 14,000*g* for 10 min. The mitochondrion-enriched pellet was suspended once more in mitochondrial isolation buffer and then centrifuged at 14,000*g* for 10 min. The pellet was resuspended in mitochondrial isolation buffer and used for an immediate respiration analysis. Just prior to respiration studies, an aliquot was used for determination of the protein concentration using a Bradford assay (Bio-Tek Instruments, Inc.) in the mitochondrion-enriched fraction, used for input in respiration assays.[17]

In some studies, aliquots of these fractions were assessed by immune blot to determine the relative enrichment of the mitochondria in the fractions. Relative to the initial homogenate, there is approximately a six- to sevenfold increase in the mitochondrial marker vs a two- to threefold increase in nuclear and endoplasmic reticulum markers, while the lysosomal marker, lysosome-associated membrane protein-1 (LAMP-1), was not observed in the final fractions (see the Supporting Information and Supporting Figure S1).

Cytochrome C Oxidase Assay. Cytochrome C oxidase activity was measured using a colorimetric assay manufactured by AMSBIO (AMSBIO LLC, Cambridge, MA). Assays were performed on mitochondrion-enriched fractions isolated as described above. Prior to performing the assay, the following conditions were tested: control, mitochondria plus 20 μM PAPS, mitochondria plus 1 nM SULT1C2 plus 20 μM PAPS, and mitochondria plus 1 μM cholesterol sulfate for 30 min. The change in absorbance at 565 nm was measured by using a CLARIOstar spectrophotometer (BMG Labtech, Cary, NC). All studies were performed in triplicate with four technical replicates for each assay condition. Statistical significance was determined by Student's *t*-test[18] with significance determined at $p < 0.05$.

Mitochondrial Respiration. Mitochondrial respiration was measured using an Oroboros Oxygraph-O2k (Oroboros Instruments, Innsbruck, Austria) as previously described.[19,20] Equivalent amounts of mitochondrial protein (1 mg per study) were loaded into a final volume of 2.0 mL of miRO5 respiration buffer (110 mM sucrose, 20 mM HEPES, 20 mM taurine, 60 mM K-lactobionate, 3 mM $MgCl_2$, 10 mM KH_2PO_4, 0.5 mM EGTA, 1 g L^{-1} bovine serum albumin, pH 7.1). Following addition of isolated mitochondria, oxygen flux was allowed to stabilize before addition of substrates or ADP. Substrates were added in the following order and diluted to the following final concentrations: 10 μM isocitrate; 2.5 μM malate; 20 nM ADP; 7.5 μM pyruvate; 20 nM ADP; 10 μM succinate; and in the final assay step, 20 nM ADP with 1 μM rotenone. For experiments in which cholesterol sulfate was

https://doi.org/10.1021/acs.biochem.3c00344
Biochemistry 2024, 63, 2310−2322

added to the assay, we added a final concentration of 10 nM to the chamber.

In studies performed to evaluate SULT1C2 activity on mitochondrial physiology, rat kidney mitochondria were prepared from naïve, untouched rats, and 50 μg of sulfotransferase was added to the reaction vessel, with or without PAPS (10 μM) (3′-phosphoadenosine 5′ phosphosulfate). Data were analyzed using Oroboros DatLab version 6 (Oroboros Instruments, Innsbruck, Austria), and calibration prior to experimentation was conducted according to Oroboros protocols.

Assessment of Cholesterol Sulfate Production by Thin-Layer Chromatography. Isolated mitochondria (2 mg) were incubated with SULT1C2 (25 μg/mg mitochondrial protein) with or without 10 μM PAPS and incubated at 37 °C for 30 min. Samples were cooled on ice and then centrifuged at 10,000*g* for 10 min. The pellet was extracted with a 2:1:0.8 mixture of chloroform/methanol/water.[21] The sample was agitated to optimize the lipid extraction, and the extract was filtered through Whatman grade 1 filter paper (Cytiva, Amersham, UK). The filtrate was transferred to a glass test tube, the upper layer was removed by aspiration, and the chloroform in the bottom layer was evaporated by passing dry N_2 over the liquid. The isolated lipids were resuspended in 100 μL of 2:1 chloroform/methanol solution. The following controls were also included in the studies: 2 μM cholesterol or cholesterol sulfate dissolved in 2:1 chloroform/methanol. To test for the ability of SULT1C2 to convert cholesterol to cholesterol sulfate in the absence of a biological membrane, cholesterol (1 μg/mL) was incubated with 25 μg of SULT1C2 and 10 μM PAPS for 30 min at 37 °C. The reaction was terminated by adding 10× volume of 2:1:0.8 mixture of chloroform/methanol/water. The lipids were isolated as described above and prepared for thin-layer chromatography analysis (see detailed methods in the Supporting Information).

Lipidomics Analysis. Equivalent amounts of mitochondrion-enriched fractions (1 mg total protein) were subjected to the following conditions: control untreated, mitochondria treated with SULT1C2 (25 μg/mg mitochondrial protein) for 60 min at 37 °C, mitochondria treated with sulfotransferase (25 μg/mg mitochondrial protein) just prior to snap freezing, mitochondria treated with SULT1C2 (25 μg/mg mitochondrial protein) plus 10 μM PAPS for 60 min at 37 °C, and mitochondria treated with 1 μM cholesterol sulfate for 5 min at 37 °C.

The mitochondrial samples were spiked with 10 μg/mL of d_7-cholesterol and 500 ng/mL of d_7-cholesterol sulfate as internal standards and then submitted to Bligh and Dyer extraction.[21] Briefly, 200 μL of the sample was transferred to a CK14 Precellys tube of 0.5 mL and homogenized using a Precellys Evolution homogenizer (Bertin Technologies SAS, France). The homogenate was transferred to a 1.5 mL tube and extracted with 1100 μL of chloroform/methanol/water in a 1:2:0.8 ratio. The sample was vortexed and centrifuged at 20,000*g* for 10 min to obtain aqueous and organic phases. The top and bottom phases were collected separately, dried under a vacuum centrifuge, and stored at −80 °C until LC−MS/MS analysis.

Extracts were resuspended with 50 μL of 3:1 methanol/chloroform, vortexed, and centrifuged, and the supernatants were transferred to LC vials. The LC−MS/MS analysis was performed in an Agilent 1290 Infinity II LC with multisampler (Agilent Technologies, San Jose, CA) coupled with a 6470 triple quadrupole mass spectrometer (Agilent Technologies, San Jose, CA) equipped with a Jet Stream ESI ion source. 10 μL of the resolubilized extract was loaded into a Waters XBridge C18 2.1 × 100 mm, 3.5 μm column (Waters Corporation, Milford, MA). The binary pump flow rate was 0.4 mL/min, and mobile phase A was 40:40:20 (v/v) of acetonitrile/methanol/water at 50 mM ammonium acetate and mobile phase B was 3:1 (v/v) of methanol/chloroform. The gradient went from 0 to 100% of B in 5 min, held at 100% for 5 min, returned to 0% B at 11 min, and re-equilibrated for 4 min.

The tandem mass spectrometer was operated in multiple reaction monitoring (MRM) mode. Concentration of cholesterol and cholesterol sulfate in μg per sample was obtained by calculating the ratio of the endogenous compound and the corresponding deuterated internal standard peak area and then multiplying by the internal standard concentration spiked. Data processing utilized Agilent Mass Hunter (Agilent, Santa Clara, CA).

Measurement of Mitochondrial Membrane Order. Mitochondrion-enriched fractions (1 mg of total protein) were incubated with a final concentration of 1 nM of human recombinant SULT1C2 protein, 10 μM PAPS (Sigma-Aldrich, St. Louis, MO), and 10 μM Laurdan (Thermo Fischer Scientific, Waltham, MA). 50 μL of this suspension was placed on a slide for fluorescence lifetime measurement (FLIM) analysis as previously described.[22,23] Prior to all studies, the FLIM module (ISS, Champaign, IL) was calibrated with coumarin dissolved in ethanol to a final concentration of 6.1 mg/mL and fluorescein dissolved in 0.01 M NaOH at a concentration of 1 mg/mL. Measured fluorescence lifetimes from the calibration studies were 2.5 ns for coumarin and 4.04 ns for fluorescein. These results agree with measured lifetimes published on the ISS Web site (www.iss.com).

Intravital Kinetic Studies of Mitochondrial Membrane Potential. Intra vital imaging of mitochondrial structure and function was evaluated using Rhodamine 123 according to methods described by Hall et al.[24] Sprague−Dawley rats transfected with either SULT1C2 or LAC-Z plasmid (as a control) were prepared for imaging, and background images were taken for 10 regions to be studied and analyzed. An 18 μg/kg b.w. dose of the mitochondrial potential dye, tetramethylrhodamine methyl ester (TMRM) (Thermo Fisher, Waltham, MA), was administered as a single bolus via a venous access line. Images from 10 selected regions were taken at 5, 15, and 30 min postinfusion for analysis. An inverted Leica SP-8, 2-photon microscope with Dive detectors (Wetzlar Germany) with a 40× water immersion objective (1.1 NA) at 1.5× zoom for a total magnification of 60× was used to collect images. MetaMorph (version 7.7.0.0, Molecular Devices, San Jose, CA) was used for the analysis.

Image analysis was performed by thresholding images to highlight the area occupied by the tubular epithelia while avoiding the interstitial and vascular spaces, the average intensity was recorded for each time point, and the background value was subsequently subtracted. The average values for each time point were then normalized to the respective 5 min value and analyzed using Student's *t*-test in Microsoft Excel (Redmond, WA).

Histological Assessment and LacZ Tissue Staining. For studies assessing levels of renal injury, bisected kidney tissue was fixed by immersion in 10% neutral buffered formalin and 4 μm sections were stained with hematoxylin/eosin

https://doi.org/10.1021/acs.biochem.3c00344
Biochemistry 2024, 63, 2310−2322

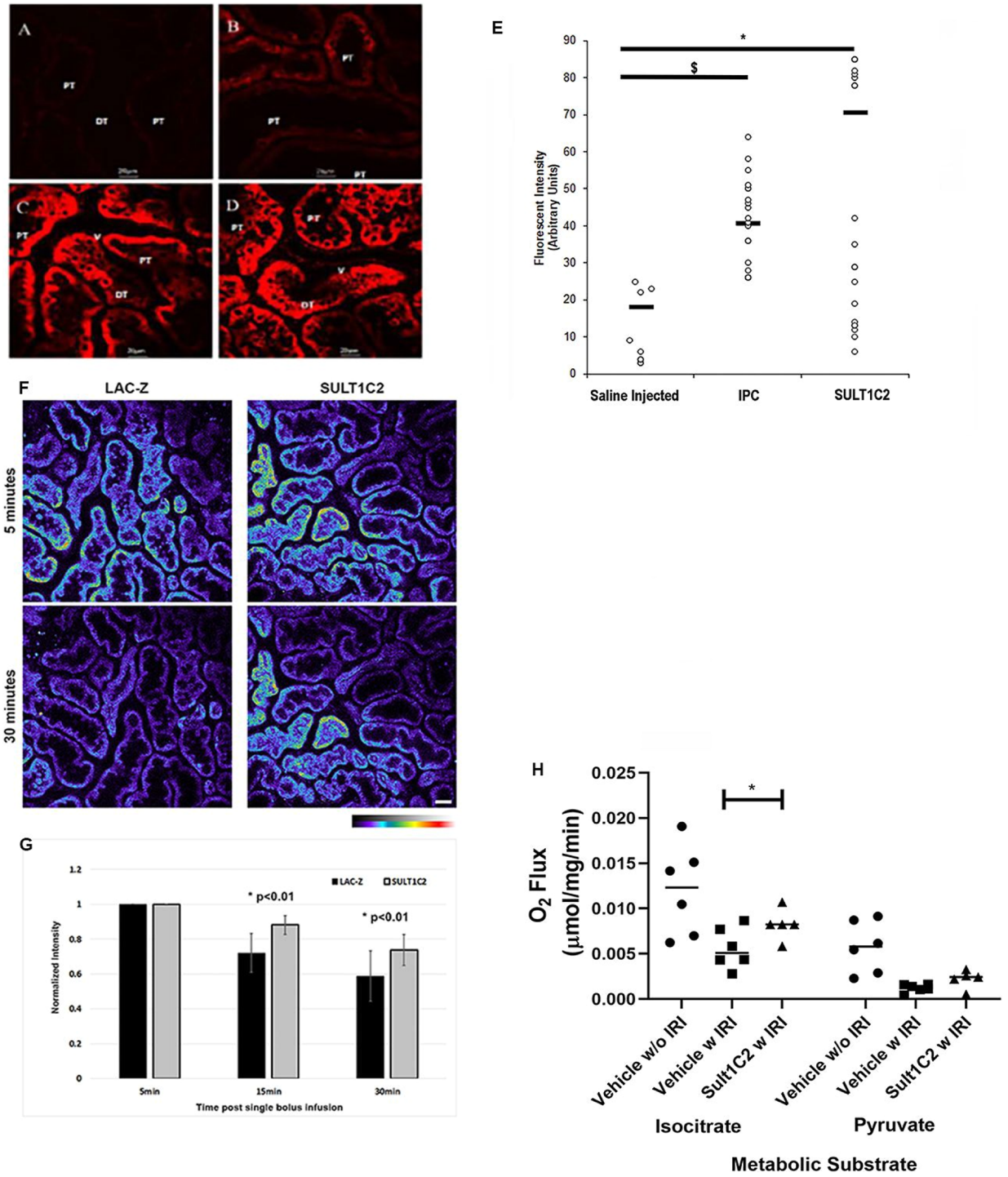

Figure 1. Mitochondrial membrane analysis following gene delivery and IPC. TMRM-labeled mitochondria by intravital microscopy in sham rats (A), rats following mock transfection (B), transfection with SULT1C2 (C), or following IPC (D). (E) Fluorescence intensity measurements compared between saline-injected kidneys (saline), IPC-treated kidneys, and SULT1C2 gene-delivered kidneys. *p value < 0.001, $$p$ value < 0.001. N = 50 for each group, bars = standard deviation. (F) 5 and 30 min post infusion of TMRM, image at 30× magnification for the LAC-Z transfected rat on the left (taken for a larger view of the renal surface). Panels on the right show a similar set of micrographs for the SULT1C2 transfected rat; a pseudo-color intensity scale bar is located below figure F. Note the significant decrease in intensity throughout the tubules in the control LAC-Z transfected rat between the first and last time point. In contrast, the SULT1C2 micrographs at 30 min show a minimal decrease in intensity. This is consistent with the experimental design. Retention of TMRM in the tubules after a single bolus will be dependent on mitochondrial potential alone; greater potential reduces loss of fluorescence over time. The graph in panel G displays the analysis of the 60× images from the 10 fields, showing a significant difference in dye retention at the 15 and 30 minute time points. Bar = 40 μm. (H) Renal cortical mitochondria isolated from saline-treated kidneys (vehicle w/o IRI), saline-treated kidneys with I/R injury or kidneys injected with plasmids encoding SULT1C2 and then subjected to I/R injury (SULT1C2 w IRI) were subsequently studied using an Oroboros O2 oxygraph. The maximum oxygen flux (OCR) in response to added pyruvate or isocitrate was measured. *p < 0.05, N = 4, comparing OCR with isocitrate added as a substrate comparing vehicle-treated kidneys to SULT1C2 plasmid DNA-treated kidneys.

https://doi.org/10.1021/acs.biochem.3c00344
Biochemistry 2024, 63, 2310−2322

staining. Analysis of renal injury was performed by a study member blinded to the treatment based on the procedure described previously.[25]

Following intravital imaging, kidneys were recovered from euthanized rats and fixed in immersion in 2% paraformaldehyde. After fixation, kidneys were bisected along the sagittal plan and passed through graded sucrose solutions ranging from 10 to 30% at 4 °C for 12 h. Kidneys were stained with X-gal staining solution composed of X-gal 1 mg/mL dissolved in dimethylformamide, 0.5 M potassium ferricyanide, and 0.5 M potassium ferrocyanide followed by washes in PBS. Kidneys were embedded in Tissue Tek O.C.T. compound (Sakura Finetek USA, Torrance, CA) on a dry ice block. 10 μm cryostat sections were placed on Fisher plus slides, dipped in 1% gelatin at 37 °C, and air-dried. The samples were post fixed with 95% ethanol, counterstained with eosin (Sigma-Aldrich, St. Louis, MO), and mounted with Permount (Fisher Scientific, Waltham, MA). Images were collected with a Leica DM 1000 LED light microscope with a DMC 4500 camera attachment with equivalent image settings via the Leica application suite (Leica Microsystems, Wetzlar, Germany).

Statistical Analysis, Randomization, and Blindness. All statistical analyses were conducted using a two-tailed unpaired Student's t-test or one-way ANOVA with Turkey's multiple comparison. All bar graphs are expressed as means ± s.d. All experiments were conducted in duplicate with at least one control group and one experimental group to ensure random assortments. Injury scoring was performed under blind conditions.

RESULTS

SULT1C2 Increases Mitochondrial Membrane Potential. Our recent study identified increased mitochondrial content of SULT1C2 in kidney following IPC by proteomic screening.[10] To verify these results, we repeated the experimental preconditioning procedure and performed immune blot analysis for SULT1C2 on isolated kidney mitochondrial fractions, using a standardized approach[26] (Supporting Information Figure S1 lanes 7 and 8). The results from these immuno blots show that SULT1C2 is enriched in the same fractions that contain cytochrome *c*. Notably, LAMP-1, an integral membrane protein located in lysosomes, is not found in the cytochrome *c*-enriched fractions or with SULT1C2-enriched fractions (Supporting Information Figure S1 lanes 7 and 8 for the cytochrome *c*, SULT1C2, and LAMP-1 blots).

To confirm the presence of SULT1C2 in mitochondrial fraction and evaluate the presence of other SULT isoforms, mitochondrion-enriched fractions from preconditioned rat kidneys were subjected to proteomic analysis and queried for the presence of members of the sulfotransferase family (see Supporting Information methods). The top peptides identified corresponded to SULT1C2 and SULT1C2A (Supporting Information Table S1). SULT1B1 was also identified in mitochondria, but the content of 1C2-related isoforms was ~11-fold higher than that of 1B1. SULT1A1 was also identified in kidney, but it was not found in the final mitochondrial fractions used for our studies (see Supporting Information Table S1). These data strongly suggest that SULT1C2 is present in the mitochondria of rat preconditioned kidneys. We also tested whether sulfotransferase 1B1 could convert mitochondrial cholesterol to cholesterol sulfate. Thin-layer chromatography analysis of the lipids extracted from mitochondria treated with sulfotransferase 1B1 or sulfotransferase 1B1 with PAPS failed to detect any cholesterol sulfate produced by the reaction (Supporting Information Figure S2A). Furthermore, we confirmed the identity of the lipid produced by SULT1C2 when incubated with mitochondria and PAPS by extracting the lipids from the labeled regions (Supporting Information Figure S2A, arrows) and analyzing the extracted lipid by lipidomics. The chromatograms are shown in Supporting Information Figure S2B and the amount of cholesterol sulfate extracted is shown in Supporting Information Table S2. The results confirm that SULT1C2 catalyzes the production of cholesterol sulfated in mitochondrial membranes. We also sought to confirm that SULT1C2 was delivered in our gene transfer experiments.

Since preconditioning alters expression of many proteins, a gene transfer approach was used to facilitate overexpression of SULT1C2 by delivery of a standard mammalian expression vector. This approach increased the expression of SULT1C2 in rat mitochondrial fractions 1 week following transfection (Supporting Information Figure S3), allowing for the potential assessment of SULT1C1 on kidney mitochondrial function without preconditioning.

To evaluate the effect of IPC or overexpression of SULT1C2 on renal mitochondrial function, we performed intravital light microscopy of kidneys following infusion of TMRM to assess the relative degree of membrane potential. Baseline fluorescence signal in sham-treated control rats or mock transfected rats displayed a low level of mitochondrial staining; however, both overexpression SULT1C2 or IPC preconditioning significantly increased the degree of fluorescence in proximal tubule relative to control values (Figure 1A–E), suggesting that both SULT1C2 or IPC increases kidney proximal tubule mitochondrial membrane potential in vivo.

These studies were repeated by comparing transfections with plasmid bearing either SULT1C2 or beta-galactosidase and evaluated TMRM fluorescence using a more rigorous kinetic analytical method.[24] This method can account for fluorescent signal decay over time due to dye transport out of the cell. Figure 1F (left upper and lower panels) and 1F (right upper and lower panels) illustrate the TMRM signal in pseudocolored blue at 5 and 30 min following TMRM administration. Consistent with the previous results, SULT1C2 gene delivery to rat kidneys resulted in enhanced TMRM in renal tubule beta-galactosidase control 30 min after infusion (Figure 1F, lower panels). We confirmed the plasmid delivery and expression of beta-galactosidase in renal tubules by X-Gal staining of kidney sections (Supporting Information Figure S4). For analysis, fluorescence intensity values were normalized for each individual animal and demonstrate a significant increase in TMRM fluorescence in SULT1C2 vs beta-galactosidase indicative of an increase in mitochondrial membrane potential (Figure 1G).

SULT1C2 Preserves Mitochondrial Function and Attenuates Injury in Response to Ischemia Reperfusion. Since mitochondrial dysfunction promotes renal proximal tubule damage following reperfusion injury, we sought to determine if alterations in mitochondrial function due to SULT1C2 expression would result in renal protection, such as IPC. I/R injury was performed on rats 1 week following delivery of the SULT1C2 expression plasmid. 24 h following I/R, serum creatinine levels rose to between 3 and 4 mg/dl on saline-injected control rats; creatinine was significantly attenuated post I/R in rats pretreated with SULT1C2

https://doi.org/10.1021/acs.biochem.3c00344
Biochemistry 2024, 63, 2310−2322

expression plasmid and was similar to sham control and the degree of protection was comparable to that observed following IPC (Figure 2A). Consistent with the effect on creatinine, SULT1C2-treated kidneys showed significant structural protection based on standard histological assessment relative to vehicle control (Figure 2B,C).

Previous studies have shown that mitochondrial respiratory capacity is significantly impaired in the early post I/R period, which is thought to set in motion cellular injury. Therefore, we sought to determine the effect of SULT1C2 transfection on mitochondrial respiration 1 h following reperfusion injury. Mitochondria from vehicle-treated rats show a significant reduction in the state-III oxygen consumption rate, 1 h following I/R relative sham (no IRI) controls when using isocitrate as a substrate. However, gene transfer significantly enhanced oxygen consumption following IRI relative to vehicle (Figure 1H). Notably the oxygen consumption rate is not significantly changed when pyruvate is the substrate (Figure 1H), suggesting that SULT1C2 affects more downstream sites in the tricarboxylic acid cycle or the efficiency of downstream complexes II and III. Taken together, these data suggest that SULT1C2 may affect resistance to injury by affecting mitochondrial function.

SULT1C2 Increases State-II/III Mitochondrial Respiration. Given the observation that SULT1C2 overexpression appears to preserve oxygen consumption, we evaluated oxygen consumption in mitochondria isolated from control rat kidneys in response to exogenous SULT1C2 exposure in vitro. Representative oxygen consumption tracings are shown for normal control mitochondria following the addition of SULT1C2 and the subsequent addition of succinate and ADP (Figure 3A,C), and the OCR did not differ from control mitochondria in the absence of added SULT1C2. However, when the sulfate donor PAPS was added to the presence of SULT1C2 , there was a threefold increase in the level of OCR (Figure 3B,C). Notably, neither SULT1C2 alone nor PAPS alone altered maximal O2 flux, but there was a statistically significant increase in maximal oxygen flux with the addition of SULT1C2 and PAPS compared to other groups (Figure 3C). These data strongly suggest that SULT1C2 alters mitochondrial respiratory function due to its sulfotransferase activity.

SULT1C2 Increases Mitochondrial Respiration by Converting Cholesterol to Cholesterol Sulfate in Mitochondrial Membranes. To determine the molecular targets of SULT1C2 in mitochondria, we initially sought to evaluate the potential mitochondrial protein tyrosine sulfation. We performed immune blots of isolated mitochondria probed with antisulfotyrosine, which revealed only one 28 kDa band, that was not changed by the following incubation with SULT1C2 and PAPS (Supporting Information Figure S5A). These observations suggest that SULT1C2 does not mediate protein sulfation and affect mitochondrial respiratory function.

Alternatively, we evaluated whether SULT1C2 could modify the mitochondrial lipid composition. We extracted mitochondrial membrane lipids as previously described and separated the lipids using thin-layer chromatography.[27] Figure 4A shows that a band of cholesterol sulfate is detected in mitochondria treated with SULT1C2 and PAPS (lane 6) while mitochondria treated with PAPS alone or SULT1C2 alone have undetectable or lower levels of cholesterol sulfate (Figure 4A lanes 4 and 5). The band observed in lane 6 has the same R_f as purified cholesterol sulfate run on a separate thin-layer chromatography plate (Figure 4A lane1 and Table 1).

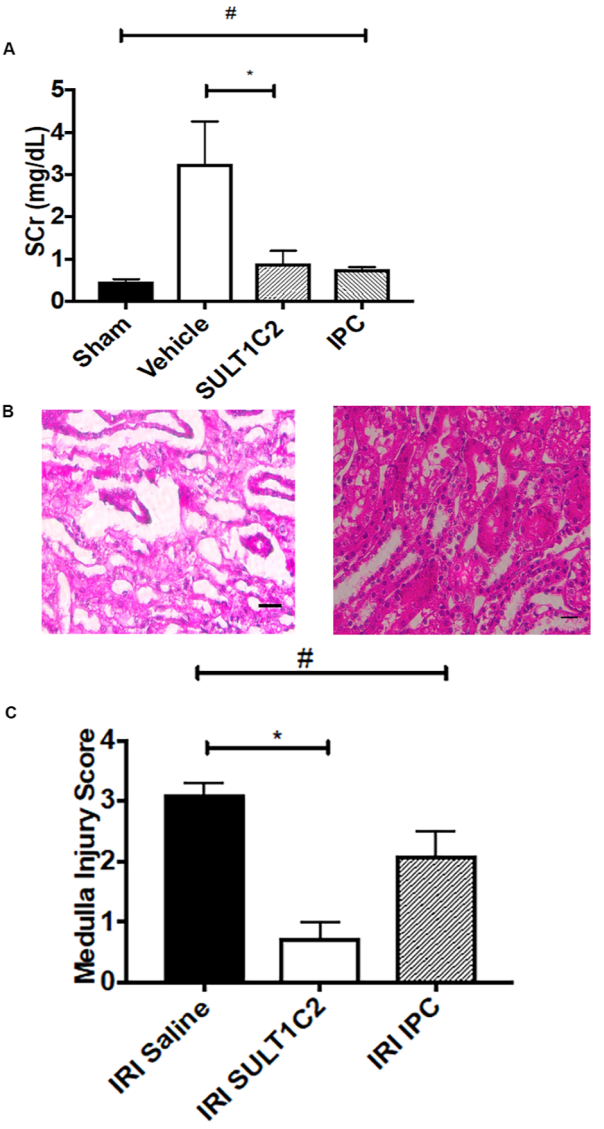

Figure 2. SULT1C2 gene delivery prevents ischemic injury. (A) Serum creatinine measurements comparison between sham, vehicle-treated, SULT1C2 gene delivery, and IPC groups. #—no statistical difference between sham, SULT1C2, and IPC groups ($N = 4$). *$p <$ 0.01 comparing vehicle and SULT1C2 groups ($N = 4$). This data shows that SULT1C2 confers protection against subsequent ischemic injury like the effect of IPC. (B) Hematoxylin and eosin staining of corticomedullary kidney junctions. Left panel: vehicle-treated kidney. Right panel: SULT1C2 transformed kidney. The vehicle-treated kidney shows signs of extensive necrosis that is missing in the SULT1C2 transformed kidney. Both kidney sections are made from tissue fixed 24 h after a 40 min renal pedicle cross-clamp-induced ischemic injury. Bar = 25 μm. (C) Medullary injury scores comparing kidney cortico-medullary regions from kidneys treated with ischemia-reperfusion injury (IRI = 40 min renal pedicle cross-clamp) 7 days after saline (vehicle) hydrodynamic delivery or SULT1C2 gene delivery. Alternatively, kidneys were subjected to IRI after a treatment 14 days before IPC. All tissues are stained with hematoxylin and eosin. A blinded reviewer determined all injury scores. *$p <$ 0.01 comparing IRI/saline vs IRI/SULT1C2 gene transduced kidneys. #$p <$ 0.05 comparing IRI/saline vs IRI/IPC kidneys. $N = 5$ for each group with three replicates. This data shows that SULT1C2 gene transduction protects against subsequent ischemic injury.

Previous studies found that SULT1C2 does not sulfate steroids.[28] Similarly, we observed that incubation of cholesterol

https://doi.org/10.1021/acs.biochem.3c00344
Biochemistry 2024, 63, 2310−2322

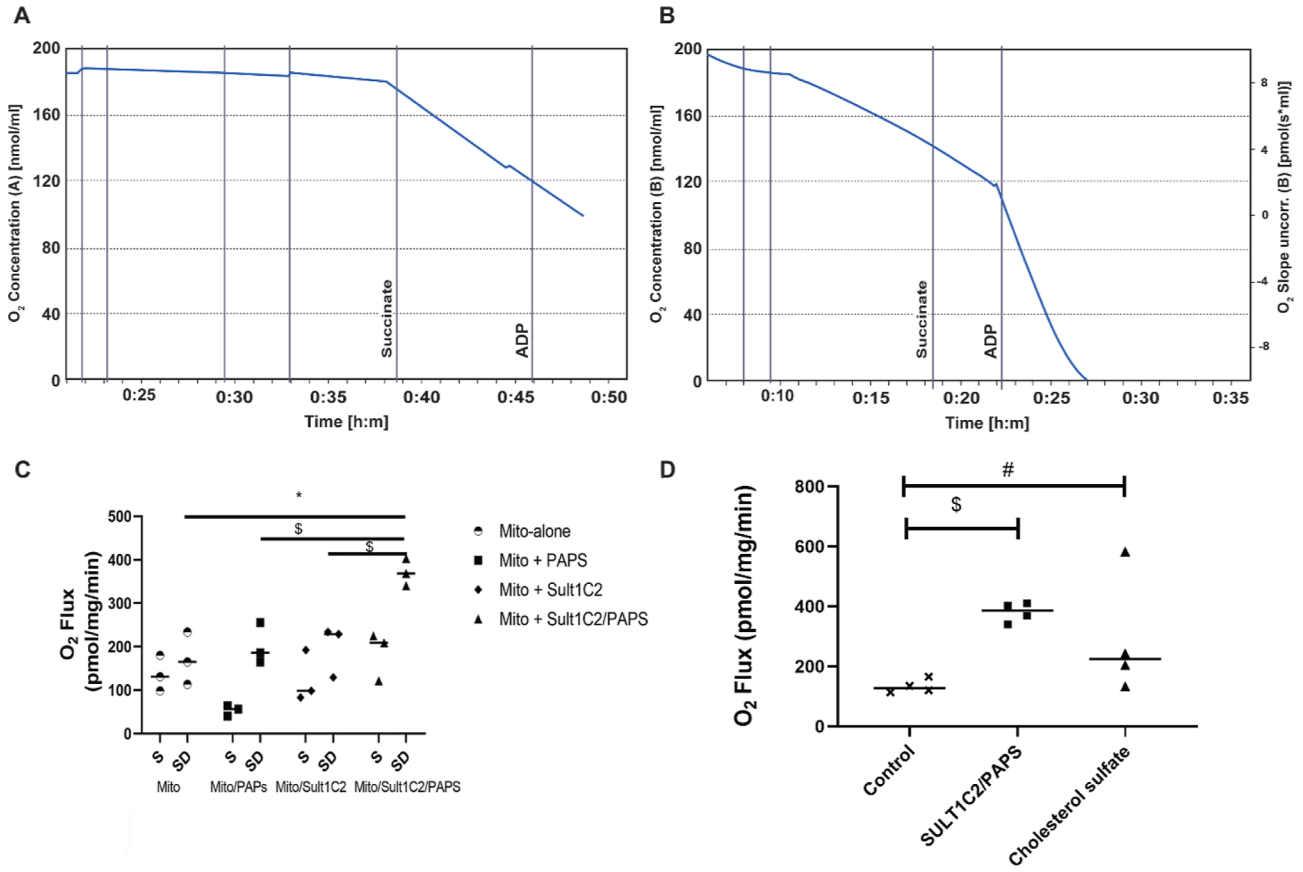

Figure 3. SULT1C2 and PAPS or cholesterol sulfate increases state-III respiration *in vitro*. Mitochondrial oxygen consumption is measured in the presence of isolated mitochondria treated with (A) SULT1C2 or (B) SULT1C2/PAPS following the addition of succinate (S) and ADP (D). (C). Measurement of mitochondrial respiration following the addition of succinate (S) or succinate/ADP (SD) in isolated mitochondria treated with vehicle, PAPS, SULT1C2, or the combination of SULT1C2/PAPS. (D). Mitochondrial respiration is also analyzed with and without the addition of 10 nM cholesterol sulfate vs vehicle. Data indicates that the addition of the cholesterol sulfate (10 nM) increases mitochondrial respiration compared to controls (*$p < 0.05$ control vs cholesterol sulfate; #$p < 0.05$ control vs SULT1C2/PAPS).

with purified SULT1C2 and PAPS does not generate cholesterol sulfate (Figure 4A lane 3), but cholesterol sulfate is formed only in the presence of mitochondrial extracts. It is possible that the limited solubility of cholesterol in water is too low for a cholesterol sulfate reaction product to be detected in our assay. Alternatively, the data may suggest that the conversion of cholesterol to cholesterol sulfate in mitochondria by SULT1C2 requires an interaction with components of mitochondria.

In separate studies, cholesterol sulfate was identified in mitochondria isolated from ischemia preconditioned kidneys (Figure 4B). This observation is strengthened by the measured R_f value ($R_f = 0.52$) of the cholesterol sulfate band in Figure 4B (Table 1) which matches the R_f value of a pure cholesterol sulfate band ($R_f = 0.52$) in Figure 4A.

To further confirm the possible sulfation of cholesterol by SULT1C2 by thin-layer chromatography, lipidomics was performed on the following experimental conditions; control untreated mitochondria, mitochondria incubated with SULT1C2 plus PAPS at 37 °C for 60 min, mitochondria incubated at 37 °C for 60 min with SULT1C2 plus PAPS spiked into the sample just prior to snap freezing, and mitochondria samples spiked with cholesterol sulfate. Evaluation of the ratio of the reaction product (cholesterol sulfate) vs the substrate (cholesterol) shows that there is a statistically significant difference in the ratio in samples treated with SULT1C2 plus PAPS for 60 min ($p < 0.03$, Table 2).

In contrast, when SULT1C2 and PAPS are added to the isolated mitochondria just prior to snap freezing the samples, the ratio of the reaction products is not statistically significantly different than control samples ($p = 0.26$, Table 2). These data support the hypothesis that SULT1C2 promotes mitochondrial cholesterol sulfate formation.

We next sought to determine whether the formation of cholesterol sulfate could alter mitochondrial respiration. We repeated assays on control isolated mitochondria and confirmed that SULT1C2 and PAPS significantly increased the oxygen consumption rate and demonstrated that addition of exogenous cholesterol sulfate, in the absence of added SULT1C2 and PAPS, also sharply elevated OCR (Figure 3D). Taken together, these data strongly suggest that SULT1C2 alters the mitochondrial respiratory activity via the production of cholesterol sulfate.

SULT1C2 Changes Mitochondrial Membrane Order. To assess the possible effects of SULT1C2 on the mitochondrial membrane, we analyzed the fluorescence lifetime of isolated mitochondria labeled with MitoTracker Red and Laurdan with and without SULT1C2 and PAPS. The mitochondria were then imaged using a confocal microscope equipped for fluorescence lifetime imaging. The phasor diagram from these studies is shown in Figure 5. The half-

https://doi.org/10.1021/acs.biochem.3c00344
Biochemistry 2024, 63, 2310−2322

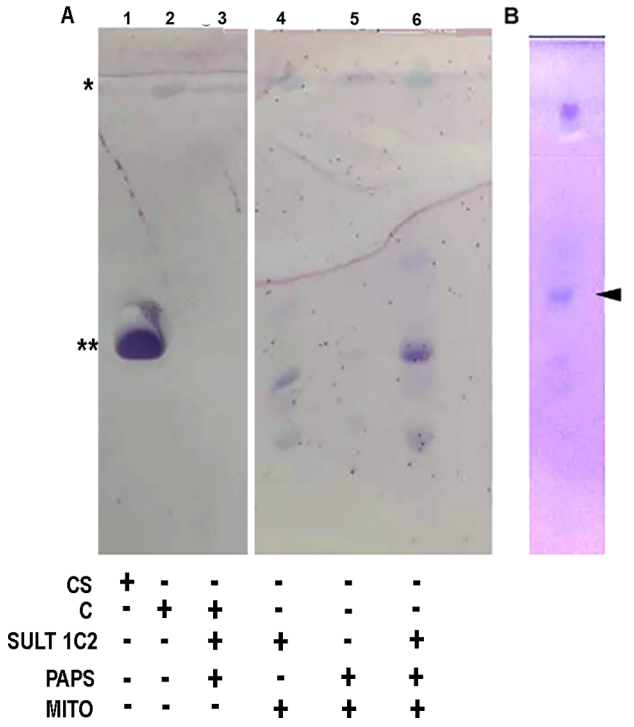

Figure 4. SULT1C2 converts cholesterol to cholesterol sulfate in mitochondrial membranes. Thin-layer chromatography analysis shows that mitochondria have cholesterol sulfate. (A) Synthesis of cholesterol sulfate by SULT1C2 is dependent on PAPS. SULT1C2 does not convert cholesterol to cholesterol sulfate in the absence of mitochondria. Conversion of mitochondrial cholesterol to cholesterol sulfate is dependent on PAPS. C: cholesterol, CS: cholesterol sulfate, MITO: mitochondria, PAPS: 3′phosphoadenosine-5-phosphosulfate, and SULT1C2: sulfotransferase 1C2. ** Cholesterol sulfate signal and region where cholesterol sulfate is expected to migrate on the thin-layer chromatography plate based on the migration of pure cholesterol sulfate. * Cholesterol signal and region where cholesterol is expected to migrate on the thin-layer chromatography plate based on the migration of pure cholesterol. (B) Mitochondria isolated from ischemia preconditioned kidneys have cholesterol sulfate in their lipid membranes. Arrowhead points to the cholesterol sulfate signal. The signal at the top of the image is cholesterol.

Table 1. Relative Migration (R_f) of Labeled Lipids

sample	R_f
cholesterol standard	0.97
cholesterol sulfate standard	0.52
control mitochondrial cholesterol band	0.95
mitochondria + SULT1C2 + PAPS cholesterol band	0.96
mitochondria + SULT1C2 + PAPS cholesterol-SO_4 band	0.48
mitochondria from IPC kidney-cholesterol band	0.94
mitochondria from IPC kidney-cholesterol sulfate band	0.52

life of fluorescence (τ) in mitochondria in the blue maximum wavelength of Laurdan is 4.12 ns. In contrast, τ is equal to 3.66 ns in mitochondria treated with SULT1C2 and PAPS ($p < 0.05$). Similarly, in the green wavelength, τ is 4.55 ns in control mitochondria and 4.48 ns ($p < 0.05$) in sulfotransferase with PAPS-treated mitochondria. Since FLIM queries the local environment of fluorophores and Laurdan shifts its fluorescence in response to changes in lipid packing, our data points to a change in the lipid membrane environment that results in a more disorganized lipid packing state.[29,30]

SULT1C2 Decreases Cytochrome C Redox Kinetics. Mitochondrial membrane potential is increased in ischemia preconditioned kidneys (Figure 1); yet, assays of isolated mitochondria from ischemia preconditioned kidneys reveal increased state-II/III respiration. Since oxidative phosphorylation will dissipate membrane potential when ATP is synthesized, in the absence of changes in uncoupling protein action, there must be a step in the ATP synthetic pathway where there is a decrease in reaction kinetics. To test this possibility, we measured the kinetics of cytochrome C reduction in mitochondria treated with and without SULT1C2 and PAPS or cholesterol sulfate. Table 3 compares reaction kinetics between control, sulfotransferase- and PAPS-treated, and cholesterol sulfate-treated mitochondria. Sulfotransferase and PAPS along with cholesterol sulfate significantly slowed cytochrome C reduction rates as compared to control mitochondria.

DISCUSSION

SULT1C2 is one of the cytoplasmic sulfotransferase enzyme family members which modify hormones, steroids, and xenobiotics using the universal sulfuryl donor, PAPS.[31,32] While sulfation is a critical component of androgen biosynthetic and triiodothyronine degradation pathways, little evidence has directly linked the action of sulfotransferase enzymes to metabolism. Shi et al. demonstrated that sulfotransferase 2B1b inhibits gluconeogenesis in hepatocytes by blocking hepatocyte nuclear factor 4 import into the nucleus.[33,34] Sulfotransferase 2B1b expression is increased in the transition from the fasted to fed state. Since sulfotransferase 2B1b coverts cholesterol to cholesterol sulfate, the effect of feeding cholesterol sulfate to obese rats was tested and found to recapitulate sulfotransferase 2B1b's inhibitory effects on gluconeogenesis.[34] Analysis of the downstream effects of cholesterol sulfate and sulfotransferase 2B1b identified a decrease in acetyl-coenzyme A synthetase, leading to a global decrease in protein acetylation with decreased acetylated hepatocyte nuclear factor 4a. This resulted in nuclear exclusion of hepatocyte nuclear factor 4a.[34] Two recent studies point to a protective role for sulfotransferase in cellular protection. Sulfotransferase 4A1, a cytosolic neuronal sulfotransferase, knockout mice exhibit early postnatal death, and there is an accumulation of reactive oxygen species in primary cortical neurons. Subcellular fractionation studies revealed the presence of sulfotransferase 4A1 in mitochondrial fractions. Furthermore, cells expressing sulfotransferase 4A1 had mitochondria that were protected against hydrogen peroxide oxidative injury and loss of membrane potential.[35] Subsequently, Brettrager et al. used yeast as a model system to study sulfotransferase 4A1 following its localization on the mitochondrial outer membrane in which its sulfating activity conferred cellular protection against oxidative injury with hydrogen peroxide.[36] Strikingly, the cellular protective action of sulfotransferase 4A1 was dependent on PAPS and extracellular sulfate.[36]

To evaluate SULT1C2's activity on mitochondria, we first tested for evidence of tyrosine sulfation in isolated mitochondria but could find no evidence of tyrosine sulfation in response to SULT1C2 (Supporting Information Figure S5). From this finding, we next considered the possibility that SULT1C2 was modifying mitochondrial membrane lipids. In our assay of cholesterol sulfate production, we found that SULT1C2 mediated the production of cholesterol sulfate only

https://doi.org/10.1021/acs.biochem.3c00344
Biochemistry 2024, 63, 2310−2322

Table 2. Effect of SULT1C2 on Cholesterol Sulfate Levels in Isolated Mitochondria

	cholesterol-SO_4 μg/sample	cholesterol μg/sample	ratio cholesterol-SO4/cholesterol × 100	P value comparing ratios to control
control sample 1	1.197	39.55	3.027	
control sample 2	1.111	38.14	2.914	
control sample 3	1.244	41.10	2.736	
control sample 4	1.122	37.33	3.007	
average of control samples	**1.14**	**39.03**	**2.92**	
SULT1C2 + PAPS sample 1	0.975	33.72	2.89	
SULT1C2 + PAPS sample 2	0.883	24.29	3.64	
SULT1C2 + PAPS sample 3	1.271	36.74	3.46	
SULT1C2 + PAPS sample 4	1.064	32.25	3.30	
average SULT1C2 + PAPS	**1.17**	**34.5**	**3.32**	**0.03**
end incubation-SULT1C2 + PAPS sample 1	1.17	34.51	3.38	
end incubation-SULT1C2 + PAPS sample 2	0.94	37.22	2.53	
end incubation-SULT1C2 + PAPS sample 3	1.13	37.30	3.02	
end incubation-SULT1C2 + PAPS sample 4	1.23	37.72	3.23	
average-end incubation group	**1.05**	**34.51**	**3.04**	**0.26**
Chol-SO_4 spike sample 1	4.95	33.62	14.72	
Chol-SO_4 spike sample 2	5.25	25.11	20.92	
Chol-SO_4 spike sample 3	4.44	36.51	12.15	
Chol-SO_4 spike sample 4	5.16	35.77	14.46	
average Chol-SO_4 spike	**4.95**	**32.73**	**15.56**	**0.003**

in the presence of mitochondria. Mixing pure SULT1C2 with PAPS and cholesterol did not result in sulfate production. This suggests that either cholesterol must be incorporated into a lipid membrane for the reaction to go forward or that mitochondria have a cofactor necessary for the reaction to occur. In all our experiments, our mitochondrial isolation method maintains the organelle's oxidative phosphorylation functionality with minimal disruption of the membrane integrity. This constraint necessitated the use of enriched mitochondrial fractions in our experiments. Since sulfotransferase 2B1b is expressed in rat kidney, this enzyme, which is known to sulfate cholesterol, could account for the cholesterol sulfate production observed in our studies.[37] However, our data eliminate this possibility based on the observation that sulfotransferase 2B1b was not found in our proteomic screen of the mitochondrial fraction (Supporting Information Table S1). Furthermore, in our assays for cholesterol sulfate production, mitochondria mixed with PAPS did not produce cholesterol sulfate (Supporting Information Figures S2A and 4). Adding PAPS to the mitochondria should have activated any contaminating sulfotransferase in the mitochondrial fraction; ergo, the production of cholesterol sulfate observed in our experiments is due to the action of SULT1C2. In experiments where SULT1C2 is incubated with intact mitochondria, the synthesis of cholesterol sulfate likely occurs on the outer membrane. While cholesterol transport in mitochondria has been shown to be dependent on Star1 proteins as part of androgen steroid biosynthesis, it is not evident whether cholesterol sulfate is similarly transported.[38] Our studies do not address what additional transport steps occur with cholesterol sulfate or its relative distribution in the mitochondrial membranes. We note additional bands in Figure 4 lane 6, but these bands were not identified because these bands have a different R_f than cholesterol sulfate in lane 1 or cholesterol in lane 2. Further studies are needed to fully understand the other lipid products observed in Figure 4 lane 6 and cholesterol sulfate's synthesis and transport in mitochondria.

In a proteomic screen evaluating long-term mitochondrial adaptations to IPC, SULT1C2 was identified with the largest interval change in expression.[10] In our studies, gene transfer of sulfotransferase to the kidney cortex resulted in increased mitochondrial membrane potential (Figure 1). SULT1C2 gene transfer also markedly attenuated the renal response to subsequent ischemia (Figure 5A). Serum creatinine increased modestly in treated kidneys, while tissue injury assessment using standard tissue injury criteria showed minimal tissue injury in SULT1C2-treated kidneys (Supporting Information Figure S3). These results are similar to our studies whereby gene transfer of isocitrate dehydrogenase-2 mimicked ischemia preconditioning.[10] However, since isocitrate dehydrogenase-2 is a mitochondrial resident protein, its potential role in IPC appeared to be more straightforward. The common finding of increased mitochondrial membrane potential in the ischemia preconditioned state and IDH2 and SULT1C2 gene transfer studies led us to probe for a direct action on mitochondria by SULT1C2.

Isolated mitochondria incubated with SULT1C2 and the sulfate donor, PAPS, had a threefold increase in maximal respiration in response to succinate and ADP substrates. In the assay conditions, we measured oxygen flux in the presence of malate, glutamate, and pyruvate suggesting an increase in state-III respiration.[39] A similar effect occurs when cholesterol sulfate is added in nanomolar concentrations to mitochondria. Taken together, our data suggest that SULT1C2 modifies mitochondrial function by changing mitochondrial membrane organization. This conclusion is reinforced by the FLIM analysis of Laurdan-labeled mitochondria. SULT1C2 with PAPS treatment significantly decreases the fluorescence lifetime of Laurdan. Shortening fluorescence lifetime can be attributed to a loss of lipid order likely because of negative charged sulfate moieties introduced into the membrane

https://doi.org/10.1021/acs.biochem.3c00344
Biochemistry 2024, 63, 2310−2322

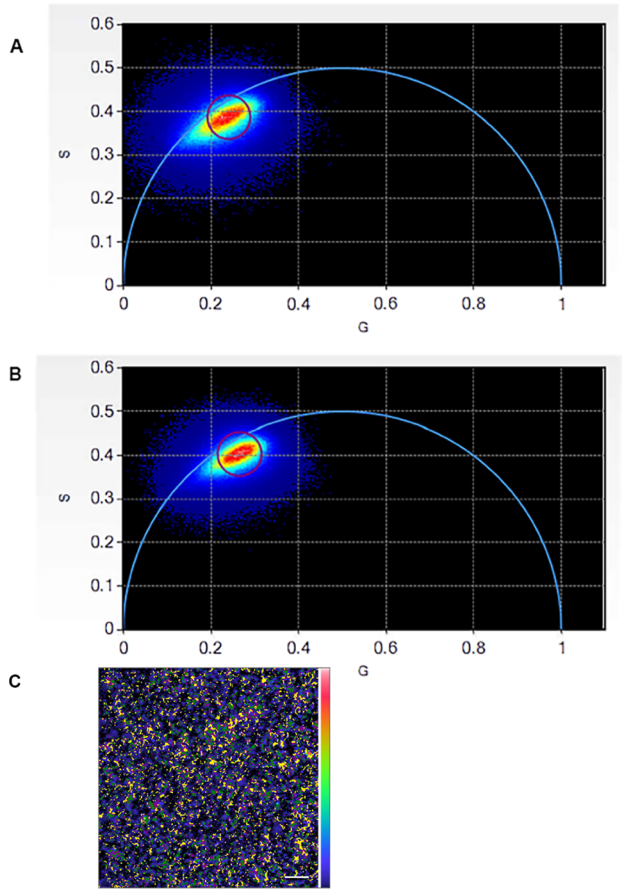

Figure 5. Fluorescence lifetime analysis of SULT1C2 and PAPS activity on mitochondrial membrane fluidity. Mitochondria were analyzed by FLIM following the addition of Laurdan, MitoTracker Red, SULT1C2, and PAPS. (A) Phasor plot of control mitochondria. (B) Phasor plot of mitochondria treated with SULT1C2 and PAPS. Phasor plots show that the addition of SULT1C2 and PAPS decreases Laurdan fluorescent lifetime, indicating potential changes in mitochondrial membrane organization. Control lifetime τ_b = 4.12 ns, τ_g = 4.55 ns vs SULT1C2-treated lifetime τ_b = 3.66 ns, τ_g = 4.48 ns ($p < 0.05$). Red circles identify the population of maximum signals collected from 10 images to determine fluorescence lifetimes (τ). (C) Image capture of MitoTracker Red stain of mitochondria analyzed by fluorescence lifetime measurements. The image is from the confocal image taken with a 580 nm excitation and emission at 644 nm. In the experiment, Laurdan fluorescence was achieved by two-photon excitation at 860 nm with emissions captured at 430−450 nm (blue) and 480−500 nm (green). Bar = 100 μm.

surface.[29,30] This likely alters mitochondrial protein complex mobility in the membrane and may account for the increase in state-III respiration.

Our data points to a counterintuitive set of findings, sulfotransferase gene transfer and IPC both increase observed mitochondrial membrane potential, yet the amount of maximum state-III-dependent oxygen consumption is elevated in mitochondria obtained from ischemic preconditioned kidney tissue or in mitochondria directly treated with SULT1C2 and PAPS. Increased rates of state-III respiration should bleed off excess membrane potential in the absence of other changes in other pathways that utilize the potential. We performed studies on ROS production and observed no changes in ROS levels in ischemia preconditioned kidneys. In immune blot studies of mitochondria complex expression, we found no changes in levels of uncoupling proteins or mitochondrial complexes. We therefore studied the rate of cytochrome C reduction and found a significant decrease in the rate of this reaction. Cytochrome C reduction is the rate-limiting step in the oxidative phosphorylation pathway; therefore, slowing this step in the oxidative phosphorylation pathway should decrease the utilization rate of membrane potential. Conversely, under conditions of substrate excess, maximal respiratory capacity is augmented.

SULT1C2 expression is regulated at the transcriptional level by vitamin D_3 response element in LS180 human adenocarcinoma colonic epithelial cells. 1α,25-Dihydroxyvitamin D3 significantly increases gene expression from the SULT1C2 PXP transcription factor binding site.[40,41] In this letter, our data shows that amplifying SULT1C2 expression either by gene transfer or by IPC confers protection against subsequent ischemic injury. By extension, we predict that vitamin D3 may be a useful pharmacologic preconditioning agent acting to enhance mitochondrial resistance to ischemic insults. However, more work will be needed to understand the kinetics of SULT1C2 expression in response to vitamin D in vivo. In summary, our observations add a new and novel mechanism of mitochondrial respiratory control.

CONCLUSIONS

In summary, in vivo observations of mitochondrial membrane potential in response to an IPC maneuver and our subsequent experimental work revealed a novel role for SULT1C2. Mitochondrion-enriched fractions from ischemia preconditioned kidneys have elevated state-III oxygen consumption compared to that of mitochondria isolated from sham control kidneys. Proteomic analysis of these mitochondrial fractions shows that SULT1C2 and 1C2A are the predominant sulfotransferase isoforms in the fractions. In studies, examining mitochondrial physiology, SULT1C2 added in combination with the high-energy sulfate donor (PAPS), increases mitochondrial state-III maximal oxygen consumption. The activation of oxygen utilization was recapitulated by the addition of cholesterol sulfate to mitochondria in physiologic studies. The evidence that SULT1C2 is converting cholesterol to cholesterol sulfate is based on lipid extraction studies using either thin-layer chromatography or a lipidomic approach. This work identifies a heretofore unknown function for SULT1C2 in cellular control of mitochondrial activity.

Table 3. Kinetics of Cytochrome *c* Reduction

sample	V_{max} (ΔOD565 nm/s) × 100	standard deviation × 100	p value compared to control
control mitochondria	1.38	0.63	N/A
mitochondria + PAPS	1.495	0.23	0.011
mitochondria + SULT1C2 + PAPS	1.58	0.45	0.012
mitochondria + cholesterol sulfate	1.58	0.21	0.007

https://doi.org/10.1021/acs.biochem.3c00344
Biochemistry 2024, 63, 2310−2322

■ ASSOCIATED CONTENT

Supporting Information

The Supporting Information is available free of charge at https://pubs.acs.org/doi/10.1021/acs.biochem.3c00344.

Immune blot analysis, thin-layer chromatography, proteomic sample preparation, LC-MS/MS analysis, immunofluorescence staining and imaging, beta-galactosidase assay for gene expression post gene delivery, proteomic analysis of fractions, immune blot analysis of mitochondrial enrichment, cholesterol sulfate chromatogram for sample 1, cholesterol chromatogram for sample 1, cholesterol sulfate produced by SULT1C2 when incubated with mitochondria and PAPS, SULT1C2 expression in kidney cortex, beta-galactosidase expression in rat kidneys, anti-sulfotyrosine blots demonstrate that sulfotyrosine 1C2 is not sulfating a mitochondrial protein, and immune localization of SULT1C2 in ischemia preconditioned rat kidney (PDF)

Accession Codes

Rat sulfotransferase 1C2 has a UniProt accession no. of Q9WUW8. Human sulfotransferase 1C2 has the UniProt accession no. of O00338.

■ AUTHOR INFORMATION

Corresponding Author

Robert L. Bacallao − *Division of Nephrology, Indiana Center for Biological Microscopy, Indiana University School of Medicine, Indianapolis, Indiana 46202, United States; Division of Nephrology, Richard Roudebush VA Medical Center, Indianapolis, Indiana 46202, United States;* orcid.org/0000-0002-5703-5701; Phone: (317)-278-0471; Email: rbacalla@iu.edu; Fax: (317)-274-8575

Authors

Alexander J. Kolb − *Department of Biology, School of Science, Indiana University-Indianapolis, Indianapolis, Indiana 46202, United States*

Peter Corridon − *Khalifa University of Science and Technology, Abu Dhabi, United Arab Emirates*

Mahbub Ullah − *Department of Anatomy, Cell Biology & Physiology, Indiana University School of Medicine, Indianapolis, Indiana 46202, United States*

Zechariah J. Pfaffenberger − *Department of Chemistry, University of Michigan, Ann Arbor, Michigan 48109, United States*

Wei Min Xu − *Division of Nephrology, Indiana Center for Biological Microscopy, Indiana University School of Medicine, Indianapolis, Indiana 46202, United States*

Seth Winfree − *Department of Pathology and Microbiology, University of Nebraska Medical Center, Omaha, Nebraska 68198, United States*

Ruben H. Sandoval − *Division of Nephrology, Indiana Center for Biological Microscopy, Indiana University School of Medicine, Indianapolis, Indiana 46202, United States*

Takeshi Hato − *Division of Nephrology, Indiana Center for Biological Microscopy, Indiana University School of Medicine, Indianapolis, Indiana 46202, United States*

Frank A. Witzmann − *Department of Anatomy, Cell Biology & Physiology, Indiana University School of Medicine, Indianapolis, Indiana 46202, United States*

Rodrigo Mohallem − *Department of Comparative Pathobiology, College of Veterinary Medicine, Bindley Bioscience Center, Purdue University, West Lafayette, Indiana 47907, United States;* orcid.org/0000-0003-3680-1291

Jackeline Franco − *IDEXX Laboratories, Westbrook, Maine 04092, United States*

Uma K. Aryal − *Department of Comparative Pathobiology, College of Veterinary Medicine, Bindley Bioscience Center, Purdue University, West Lafayette, Indiana 47907, United States; Purdue Proteomics Facility, Bindley Biosciences Center, Purdue University, West Lafayette, Indiana 47907, United States;* orcid.org/0000-0003-4543-1536

Simon J. Atkinson − *Department of Neuroscience, Physiology and Behavior, University of California, Davis, California 95616, United States*

David P. Basile − *Department of Anatomy, Cell Biology & Physiology, Indiana University School of Medicine, Indianapolis, Indiana 46202, United States*

Complete contact information is available at: https://pubs.acs.org/10.1021/acs.biochem.3c00344

Author Contributions

‡‡D.P.B. and R.L.B. contributed equally to this work.

Notes

The authors declare no competing financial interest.

■ ACKNOWLEDGMENTS

The authors thank Dr. Robert Harris (Kansas University) and Dr. Kurt Amsler (New York Institute of Technology) for their helpful suggestions. R.L.B. is a recipient of a VA Merit Award (BX-001736) and a grant from NIDDK DK-079312. D.P.B. is a recipient of the NIH award DK- 063114. R.L.B. dedicates this manuscript to Dr. William Wickner, Dartmouth Medical School, Hannover, NH, for his mentorship. This material is based upon work supported (or supported in part) by the Department of Veterans Affairs, Veterans Health Administration, Office of Research and Development. The views expressed in this article are those of the authors and do not necessarily reflect the position or policy of the Department of Veterans Affairs or the United States government.

■ REFERENCES

(1) Murry, C. E.; Jennings, R. B.; Reimer, K. A. Preconditioning with ischemia: a delay of lethal cell injury in ischemic myocardium. *Circulation* **1986**, *74*, 1124−1136.

(2) Islam, C. F.; Mathie, R. T.; Dinneen, M. D.; Kiely, E. A.; Peters, A. M.; Grace, P. A. Ischaemia-reperfusion injury in the rat kidney: the effect of preconditioning. *Br. J. Urol.* **1997**, *79*, 842−847.

(3) Athanasiadis, D.; Kapelouzou, A.; Martikos, G.; Katsimpoulas, M.; Schizas, D.; Vasdekis, S. N.; Kostakis, A.; Liakakos, T. D.; Lazaris, A. M. Remote Ischemic Preconditioning May Attenuate Renal Ischemia-Reperfusion Injury in a Porcine Model of Supraceliac Aortic Cross-Clamping. *J. Vasc. Res.* **2015**, *52*, 161−171.

(4) Gill, R.; Kuriakose, R.; Gertz, Z. M.; Salloum, F. N.; Xi, L.; Kukreja, R. C. Remote ischemic preconditioning for myocardial protection: update on mechanisms and clinical relevance. *Mol. Cell. Biochem.* **2015**, *402*, 41−49.

(5) Hussein, A. M.; Sakr, H. F.; Alenzi, F. Q. Possible Underlying Mechanisms of the Renoprotective Effect of Remote Limb Ischemic Preconditioning Against Renal Ischemia/Reperfusion Injury: A Role of Osteopontin, Transforming Growth Factor-Beta and Survivin. *Nephron* **2016**, *134*, 117−129.

(6) Liem, D. A.; Honda, H. M.; Zhang, J.; Woo, D.; Ping, P. Past and present course of cardioprotection against ischemia-reperfusion injury. *J. Appl. Physiol.* **2007**, *103*, 2129−2136.

(7) Robert, R.; Vinet, M.; Jamet, A.; Coudroy, R. Effect of non-invasive remote ischemic preconditioning on intra-renal perfusion in volunteers. *J. Nephrol.* **2016**, *30*, 393−395.
(8) Tamareille, S.; Mateus, V.; Ghaboura, N.; Jeanneteau, J.; Croué, A.; Henrion, D.; Furber, A.; Prunier, F. RISK and SAFE signaling pathway interactions in remote limb ischemic perconditioning in combination with local ischemic postconditioning. *Basic Res. Cardiol.* **2011**, *106*, 1329−1339.
(9) Wojtovich, A. P.; Nadtochiy, S. M.; Brookes, P. S.; Nehrke, K. Ischemic preconditioning: the role of mitochondria and aging. *Exp. Gerontol.* **2012**, *47*, 1−7.
(10) Kolb, A. L.; Corridon, P. R.; Zhang, S.; Xu, W.; Witzmann, F. A.; Collett, J. A.; Rhodes, G. J.; Winfree, S.; Bready, D.; Pfeffenberger, Z. J.; Pomerantz, J. M.; Hato, T.; Nagami, G. T.; Molitoris, B. A.; Basile, D. P.; Atkinson, S. J.; Bacallao, R. L. Exogenous Gene Transmission of Isocitrate Dehydrogenase 2 Mimics Ischemic Preconditioning Protection. *J. Am. Soc. Nephrol.* **2018**, *29*, 1154−1164.
(11) Stanley, E. L.; Hume, R.; Visser, T. J.; Coughtrie, M. W. Differential expression of sulfotransferase enzymes involved in thyroid hormone metabolism during human placental development. *J. Clin. Endocrinol. Metab.* **2001**, *86*, 5944−5955.
(12) Alnouti, Y.; Klaassen, C. D. Tissue distribution and ontogeny of sulfotransferase enzymes in mice. *Toxicol. Sci.* **2006**, *93*, 242−255.
(13) Schindelin, J.; Arganda-Carreras, I.; Frise, E.; Kaynig, V.; Longair, M.; Pietzsch, T.; Preibisch, S.; Rueden, C.; Saalfeld, S.; Schmid, B.; Tinevez, J. Y.; White, D. J.; Hartenstein, V.; Eliceiri, K.; Tomancak, P.; Cardona, A. Fiji: an open-source platform for biological-image analysis. *Nat. Methods* **2012**, *9*, 676−682.
(14) Bonventre, J. V.; Basile, D.; Liu, K. D.; McKay, D.; Molitoris, B. A.; Nath, K. A.; Nickolas, T. L.; Okusa, M. D.; Palevsky, P. M.; Schnellmann, R.; Rys-Sikora, K.; Kimmel, P. L.; Star, R. A. AKI: A Path Forward. *Clin. J. Am. Soc. Nephrol.* **2013**, *8*, 1606−1608.
(15) Corridon, P. R.; Rhodes, G. J.; Leonard, E. C.; Basile, D. P.; Gattone, V. H.; Bacallao, R. L.; Atkinson, S. J. A method to facilitate and monitor expression of exogenous genes in the rat kidney using plasmid and viral vectors. *Am. J. Physiol. Ren. Physiol.* **2013**, *304*, F1217−F1229.
(16) Collett, J.; Corridon, P.; Mehrotra, P.; Kolb, A.; Rhodes, G.; Miller, C.; Molitoris, B.; Pennington, J.; Sandoval, R.; Atkinson, S.; Campos-Bilderback, S.; Basile, D.; Bacallao, R. Hydrodynamic Isotonic Fluid Delivery Ameliorates Moderate-to-Severe Ischemia-Reperfusion Injury in Rat Kidneys. *J. Am. Soc. Nephrol.* **2017**, *28*, 2081−2092.
(17) Bradford, M. M. A rapid and sensitive method for the quantitation of microgram quantities of protein utilizing the principle of protein-dye binding. *Anal. Biochem.* **1976**, *72*, 248−254.
(18) Gosset, W. S. The probable error of a mean. *Biomtrika* **1908**, *6*, 1−25.
(19) Gnaiger, E. Capacity of oxidative phosphorylation in human skeletal muscle: new perspectives of mitochondrial physiology. *Int. J. Biochem. Cell Biol.* **2009**, *41*, 1837−1845.
(20) Lores-Arnaiz, S.; Lombardi, P.; Karadayian, A. G.; Orgambide, F.; Cicerchia, D.; Bustamante, J. Brain cortex mitochondrial bioenergetics in synaptosomes and non-synaptic mitochondria during aging. *Neurochem. Res.* **2016**, *41*, 353−363.
(21) Bligh, E. G.; Dyer, W. J. A rapid method for total lipid extraction and purification. *Can. J. Biochem. Physiol.* **1959**, *37*, 911−917.
(22) Hato, T.; Winfree, S.; Dagher, P. C. Intravital imaging of the kidney. *Methods* **2017**, *128*, 33−39.
(23) Hato, T.; Winfree, S.; Day, R.; Sandoval, R. M.; Molitoris, B. A.; Yoder, M. C.; Wiggins, R. C.; Zheng, Y.; Dunn, K. W.; Dagher, P. C. Two-Photon Intravital Fluorescence Lifetime Imaging of the Kidney Reveals Cell-Type Specific Metabolic Signatures. *J. Am. Soc. Nephrol.* **2017**, *28*, 2420−2430.
(24) Hall, A. M.; Rhodes, G. J.; Sandoval, R. M.; Corridon, P. R.; Molitoris, B. A. In vivo multiphoton imaging of mitochondrial structure and function during acute kidney injury. *Kidney Int.* **2013**, *83*, 72−83.
(25) Basile, D. P.; Dwinell, M. R.; Wang, S. J.; Shames, B. D.; Donohoe, D. L.; Chen, S.; Sreedharan, R.; Van Why, S. K. Chromosome substitution modulates resistance to ischemia reperfusion injury in Brown Norway rats. *Kidney Int.* **2013**, *83*, 242−250.
(26) Kolb, A. L.; Corridon, P. R.; Zhang, S.; Xu, W.; Witzmann, F. A.; Collett, J. A.; Rhodes, G. J.; Winfree, S.; Bready, D.; Pfeffenberger, Z. J.; Pomerantz, J. M.; Hato, T.; Nagami, G. T.; Molitoris, B. A.; Basile, D. P.; Atkinson, S. J.; Bacallao, R. L. Exogenous Gene Transmission of Isocitrate Dehydrogenase 2 Mimics Ischemic Preconditioning Protection. *J. Am. Soc. Nephrol.* **2018**, *29*, 1154−1164.
(27) Scandroglio, F.; Loberto, N.; Valsecchi, M.; Chigorno, V.; Prinetti, A.; Sonnino, S. Thin layer chromatography of gangliosides. *Glycoconj. J.* **2009**, *26*, 961−973.
(28) Xiangrong, L.; Jöhnk, C.; Hartmann, D.; Schestag, F.; Krömer, W.; Gieselmann, V. Enzymatic properties, tissue-specific expression, and lysosomal location of two highly homologous rat SULT1C2 sulfotransferases. *Biochem. Biophys. Res. Commun.* **2000**, *272*, 242−250.
(29) Golfetto, O.; Hinde, E.; Gratton, E. Laurdan fluorescence lifetime discriminates cholesterol content from changes in fluidity in living cell membranes. *Biophys. J.* **2013**, *104*, 1238−1247.
(30) Golfetto, O.; Hinde, E.; Gratton, E. The Laurdan spectral phasor method to explore membrane micro-heterogeneity and lipid domains in live cells. *Methods Mol. Biol.* **2015**, *1232*, 273−290.
(31) Coughtrie, M. W. H. Function and organization of the human cytosolic sulfotransferase (SULT) family. *Chem. Biol. Interact.* **2016**, *259*, 2−7.
(32) Gamage, N.; Barnett, A.; Hempel, N.; Duggleby, R. G.; Windmill, K. F.; Martin, J. L.; McManus, M. E. Human sulfotransferases and their role in chemical metabolism. *Toxicol. Sci.* **2006**, *90*, 5−22.
(33) Bi, Y.; Shi, X.; Zhu, J.; Guan, X.; Garbacz, W. G.; Huang, Y.; Gao, L.; Yan, J.; Xu, M.; Ren, S.; Ren, S.; Liu, Y.; Ma, X.; Li, S.; et al. Regulation of Cholesterol Sulfotransferase SULT2B1b by Hepatocyte Nuclear Factor 4α Constitutes a Negative Feedback Control of Hepatic Gluconeogenesis. *Mol. Cell. Biol.* **2018**, *38*, No. e00654-17.
(34) Shi, X.; Cheng, Q.; Xu, L.; Yan, J.; Jiang, M.; He, J.; Xu, M.; Stefanovic-Racic, M.; Sipula, I.; O'Doherty, R. M.; Ren, S.; Xie, W. Cholesterol sulfate and cholesterol sulfotransferase inhibit gluconeogenesis by targeting hepatocyte nuclear factor 4α. *Mol. Cell. Biol.* **2014**, *34*, 485−497.
(35) Hossain, M. I.; Marcus, J. M.; Lee, J. H.; Garcia, P. L.; Gagné, J. P.; Poirier, G. G.; Falany, C. N.; Andrabi, S. A. Sult4A1 Protects Against Oxidative-Stress Induced Mitochondrial Dysfunction in Neuronal Cells. *Drug Metab. Dispos.* **2019**, *47*, 949−953.
(36) Brettrager, E. J.; Meehan, A. W.; Falany, C. N.; van Waardenburg, R. C. A. M. Sulfotransferase 4A1 activity facilitates sulfate-dependent cellular protection to oxidative stress. *Sci. Rep.* **2022**, *12*, 1625.
(37) Kohjitani, A.; Fuda, H.; Hanyu, O.; Strott, C. A. Cloning, characterization and tissue expression of rat SULT2B1a and SULT2B1b steroid/sterol sulfotransferase isoforms: divergence of the rat SULT2B1 gene structure from orthologous human and mouse genes. *Gene* **2006**, *367*, 66−73.
(38) Mesmin, B. Mitochondrial lipid transport and biosynthesis: A complex balance. *J. Cell Biol.* **2016**, *214*, 9−11.
(39) Pesta, D.; Gnaiger, E. High-resolution respirometry: OXPHOS protocols for human cells and permeabilized fibers from small biopsies of human muscle. *Methods Mol. Biol.* **2012**, *810*, 25−58.
(40) Barrett, K. G.; Fang, H.; Kocarek, T. A.; Runge-Morris, M. Transcriptional Regulation of Cytosolic Sulfotransferase 1C2 by Vitamin D Receptor in LS180 Human Colorectal Adenocarcinoma Cells. *Drug Metab. Dispos.* **2016**, *44*, 1431−1434.
(41) Rondini, E. A.; Pant, A.; Kocarek, T. A. Transcriptional Regulation of Cytosolic Sulfotransferase 1C2 by Intermediates of the

https://doi.org/10.1021/acs.biochem.3c00344
Biochemistry 2024, 63, 2310−2322

Cholesterol Biosynthetic Pathway in Primary Cultured Rat Hepatocytes. *J. Pharmacol. Exp. Ther.* **2015**, *355*, 429−441.

https://doi.org/10.1021/acs.biochem.3c00344
Biochemistry 2024, 63, 2310−2322